Supporting Information

Fitz et al. 10.1073/pnas.1602764113

SI Text

Generating Transcription Elongation Complexes. The RNA polymerase II used in all transcription experiments was purified from *Saccharomyces cerevisiae* according to (15). Pol II was biotinylated at the amino terminus of the Rpb3 subunit for use in our setup (27). Pol II transcription elongation complexes (TECs) were generated with a stepwise assembly protocol (15, 16). Polymerases were incubated with an RNA/DNA hybrid (RNA primer annealed to the template DNA strand), followed by the addition of the nontemplate DNA strand (NDS). TECs were subsequently ligated to an ∼2-kb upstream double-stranded DNA template (labeled with a digoxigenin) and an ∼1-kb downstream double-stranded DNA template. The upstream DNA template was generated via PCR from plasmid pEG2, which has a uniform GC content (28). The active site of Pol II is located such that 71 bp of the TEC add to the downstream template transcribed by the enzyme (Fig. S2). The different downstream templates are introduced below.

Generating Nucleosomal Templates. All four canonical yeast core histone proteins were expressed and purified from *E. coli*. These histone molecules are artificial as they lack any type of post-translational modification. Nucleosomes were loaded onto the strong NPSs Widom601 (12) using salt dialysis reconstitution. The use of this artificial NPS is crucial for our experiments as it ensures exact and reproducible positioning of the nucleosomes along the downstream templates. Protocols for the histone purification and for the chromatin reconstitution were adapted from refs. 13 and 14. All nucleosome reconstitutions were done with the same batch of yeast histone octamers. The different nucleosomal templates used in this study differ in the number of high-affinity Widom601 sequences, as well as in the spacing between them (Fig. S2). Two adjacent 601 NPSs (each 197 bp) result in a spacing of exactly 50 bp between the two nucleosomes. Internucleosomal spacings of 45 or 99 bp were obtained by removing 5 bp or adding 49 bp to the 50-bp linker, respectively. A fresh PCR of the corresponding DNA template was done before every nucleosome reconstitution. The PCR products were purified and concentrated by phenol-chloroform extraction, followed by ethanol precipitation. The purified DNA templates were further cut with BstXI for further ligation to the TEC. After heat inactivating the enzyme, the cut products were purified with the Wizard SV Gel and PCR Clean-Up System (Promega). The purified DNA templates were further used for nucleosome assembly. Correct positioning of the nucleosomes on the respective templates was tested by analytical restriction digest and a subsequent gel-based assay (Fig. S1*A*). Furthermore, the reconstitution efficiency of different nucleosomal templates was tested by performing force–extension measurements (Fig. S1*B*). The TEC was then ligated to both the upstream template and the downstream template in a single ligation reaction using the Quick Ligase (NEB). At least two independent nucleosome reconstitutions were tested for each condition: 1×NPS = 4; 2×NPS (99) = 3; 2×NPS (50) = 7; and 2×NPS (45) = 2.

Force–Extension Measurements: Determining Reconstitution Efficiencies. All DNA templates to be tested were prepared as explained above, yet no polymerase was assembled onto the TEC, and instead, downstream DNA templates were equipped with a biotin tag. Before optical tweezers experiments, DNA molecules were bound to functionalized polystyrene beads. DNA tethers were formed between the biotinylated downstream DNA attached to a streptavidin coated bead (2.1 μm diameter) on one side and the digoxigenin-labeled upstream DNA template bound to an anti–digoxigenin-coated bead (2.1 μm diameter) on the other side. All experiments were performed in transcription buffer [20 mM Hepes (pH 7.6 at 20 °C), 60 mM $(NH_4)_2$ SO_4, 8 mM Mg_2 SO_4, 10 μM $ZnCl_2$, 10% (wt/vol) glycerol] supplemented with an oxygen scavenger system (29). After successful DNA tether formation between the two beads (at forces ≤ 2 pN), one optical trap was moved in a stepwise manner away from the second trap (5 nm every 200 ms), constantly increasing the load acting on the DNA template. The loading rate was ∼0.46 pN/s for the lower force range up to 5 pN, ∼0.53 pN/s for the force range between 5 and 10 pN and ∼0.62 pN/s for the force range between 10 and 16 pN. At these loading rates, the system is supposed to be at equilibrium. On increasing the load on the DNA template, individual nucleosomes unwrapped. Most of the nucleosomes were unwrapped after having reached a force of ∼15 pN. We did not observe a clear signature of the outer unwrapping event of the H2A/H2B dimers. Under the prevalent salt concentration of 60 mM $(NH_4)_2$ SO_4 (ionic strength of 120 mM), only the inner unwrapping event was observed, which is reflected in a sudden decrease in force and instantaneous increase in the extension (3, 5, 30, 31). The estimated average length increase for each event calculated from all conditions was on the order of ∼25 nm (∼74 ± 1 bp, mean ± SD). Force–extension measurements allow to determine the quality of the chromatin reconstitutions; 75% of all tested single nucleosomal templates exhibited one or more unwrapping events (68% showed a single unwrapping event), whereas for dinucleosomal templates, two or more unwrapping events were seen for ∼68–71% of all tested templates (55–59% showed exactly two unwrapping events; Fig. S1*B*).

Single-Molecule Optical Tweezers Transcription Assay. Similar to force–extension experiments, tethers were formed between the biotinylated polymerase attached to a streptavidin coated bead (2.1 μm diameter) on one side and the digoxigenin-labeled upstream DNA template bound to an anti–digoxigenin-coated bead (2.1 μm diameter) on the other side. Experiments were performed with 1 mM NTP in transcription buffer [20 mM Hepes (pH 7.6 at 20 °C), 60 mM $(NH_4)_2$ SO_4, 8 mM Mg_2 SO_4, 10 μM $ZnCl_2$, 10% (wt/vol) glycerol] supplemented with an oxygen scavenger system (29). All experiments were performed in the assisting force mode, whereby the force is applied into the direction of polymerase translocation. The force was manually set to ∼12 pN at the beginning of each experiment. We do not have a force feedback in our transcription experiments. Consequently, during active elongation the applied force decreases while at the same time the distance between the two beads increases. The force applied on the polymerase for the entire length of the experiment was kept between 12 and 4 pN.

Data Acquisition and Analysis. Data collected from optical tweezers experiments was further analyzed using a custom software written in Matlab (MathWorks; R2013b). The force data were filtered with a Gaussian filter (time constant of 1 s) or a third-order Savitzky–Golay filter (time constant of 2 s). To determine the exact distance in base pairs between the two beads, the extensible worm-like chain model (eWLC) was applied on the force data (32). For transcription experiments, the velocity was calculated as the derivative of the Gaussian-filtered signal (5, 20, 33, 34). Pauses were detected as parts of transcription traces with dwell times longer than the pause threshold (three times the mean dwell time, using the Savizky–Golay filtered data) (35). We analyzed pause densities, calculated as the average number of

pauses per kbp, and pause durations, calculated as the average duration of pauses lasting between 1 and 145 s (35).

For force–extension experiments, the force data were filtered with a Savizky–Golay filter. To determine nucleosome unwrapping events, the constantly increasing force signal was scanned for a sudden drop in force. We assigned the corresponding force and position values of the peaks and subsequent valleys to each unwrapping event.

Alignment of Single-Molecule Transcription Traces. For transcription experiments carried out on bare DNA, we assumed that most polymerases reached the end of the DNA template. Therefore, the experimental run-off length should match the template length. All used DNA templates underwent a quality check by gel electrophoresis before their use in single-molecule experiments. However, in our experiments, the run-off length deviated from the expected run-off length on average by 7.1% (~67 bp for the bare DNA template with one NPS). We ascribe these uncertainties to calibration errors, mostly caused by the spread in bead size, viscosity, and temperature. To correct for the length difference, all bare DNA trajectories were linearly scaled to the expected run-off length (3). For transcription experiments performed on nucleosomal templates, however, it is uncertain whether the polymerases reach the end of the template. The presence of a nucleosome can alter the Pol II transcription performance in a way that leads to an early transcriptional arrest due to the increased transcriptional barrier (3, 5). Only transcription trajectories where the difference between the measured and the expected run-off length was smaller than 10% were considered as trajectories where the polymerases reached the final length. All trajectories fulfilling these criteria were linearly scaled to the expected run-off length. To correct for the length uncertainty of transcription traces, where the expected run-off length was larger than the 10% cutoff, we computed a correction factor from the mean run-off length of all runs that were below the 10% cutoff (ratio between mean experimental run-off length and expected run-off length). Correction factors were computed for each nucleosomal template separately. All of the runs with the expected run-off length above the cutoff value were then linearly scaled by the respective correction factor.

Evaluation of Transcription Traces. We consider the core region consisting of 147 bp of DNA wrapped around a histone octamer plus additional flanking regions upstream and downstream of the respective region, as previously reported in Bintu et al. (3) (Fig. 1*B*), as the region of nucleosomal influence. Force–extension experiments on different nucleosomal templates revealed a reconstitution efficiency between 68% and 75%. Consequently, it is necessary to test for the presence of nucleosome on each template used in the optical tweezer. However, due to the geometry of the setup we cannot control for the presence of a nucleosome on the respective NPS on our DNA templates before the transcription experiment, because nucleosomes are not under tension at the beginning of our experiment. Furthermore, it is not possible to reliably determine the presence of a nucleosome after the nucleosome was passed (5). We find that in less than 10% of the cases where we performed postpassage force–extension measurements we observed sudden drop in force, characteristic for a nucleosomal unwrapping event, consistent with what was seen in ref. 5. These numbers compare unfavorably to the reconstitution efficiencies that were independently measured in the optical trap (Fig. S1*B*), and postpassage force extension cannot be used to test for the presence of a nucleosome. The low percentage of postpassage nucleosomal unwrapping is most probably due to the fact that tension is continuously applied and nucleosomes are probably unable to rewrap after passage. For these reasons, we decided to use the distinct increase in pausing and the characteristic slowdown of Pol II that is observed when a nucleosome is present on the DNA template (Fig. 1 *C*–*F*) (5) as a method for detecting the presence of the first nucleosome. Note, however, that we cannot use similar criteria to detect the second nucleosome, as transcriptional dynamics after passage of the first nucleosome cannot be accurately quantified in our system. This inaccuracy is because we calibrate our optical tweezers with a histone-free double-stranded DNA tether, where the nucleosomes are initially in a region that is not under tension (Fig. 1*A*). However, after nucleosomal passage, the tether between the two beads might no longer be nucleosome free, and residual interaction of histones with the upstream DNA or changes in the wrapping state prohibit a correct distance determination. However, our overall reconstitution efficiencies are reasonably high (Fig. S1*B*): 75% of all tested single nucleosomal templates had at least one nucleosome present, and 68–71% of all tested dinucleosomal templates showed at least two nucleosomal unwrapping events (Fig. S1*B*). Nonetheless, our inability to check for the presence of the second nucleosome results in a slight underestimation of the influence of the second nucleosome on the Pol II passage probability through the first nucleosomal region, because in some of the cases a second nucleosome was absent.

As an unbiased method for determining whether there was a nucleosome incorporated at the first nucleosomal region, we compared Pol II passage times through the nucleosomal region on the bare DNA template to passage times through the same region on nucleosomal templates. As a cutoff, we took the mean passage time through the nucleosomal region on the bare DNA template plus 2 SDs ($11.2 + 2 \times 1.9$ s). Each first nucleosomal region of each trajectory was evaluated individually. Passage times above the cutoff were considered to result from the presence of a nucleosome (Fig. S3*A*). Only transcription data where the first nucleosome has been present on the template were included into the subsequent analysis.

The presence of a nucleosome increases Pol II arrest probabilities in the nucleosomal region (3, 5). However, there is a spread in final arrest duration among the polymerases that arrest in the first nucleosomal region, also because there is the possibility of a sudden rip of the DNA tether between the two beads. For these cases, it is unclear whether these polymerases were indeed arrested, i.e., transcriptionally inactive, or whether they would have resumed to transcribe after some further time if the tether had not ripped. Therefore, another quality check was performed on the arrest duration within the first nucleosomal region. Only polymerases that have resided within the first nucleosomal region above a certain time threshold were included in the analysis. To determine whether a final pause within the first nucleosomal region can be considered long enough, we compared the passage times through the entire nucleosomal region of transcription trajectories collected on the single nucleosomal template to the ones of the first nucleosomal region of all trajectories of all other conditions. The cutoff time was calculated from all data (mononucleosomal template) that were previously selected for the presence of a single nucleosome and where the polymerase transcribed past the nucleosome. We took the mean passage time through this region plus 2 SDs ($66.04 + 2 \times 39.68$ s) as a cutoff time and compared it to the passage time through the first nucleosomal region of each individual run of all conditions (Fig. S3*B*). We considered that all polymerases with passage times above the cutoff value resided long enough in the first nucleosomal region and hence were included in the analysis. Note that changing the cutoff to mean + 1 SD (105 s) does not change our general results (Fig. S4*A*).

The analysis of transcription trajectories along different nucleosomal templates is therefore based on the following criteria:

Only transcription traces where the first nucleosome was present were included for further analysis;

For the polymerases that did not pass the first nucleosomal region, only those traces with passage times longer than the cutoff time of 145 s were considered;

We only consider changes in Pol II transcription dynamics within the first nucleosomal region; and

Only a time window of 145 s after encountering the first nucleosome was considered for the final analysis of Pol II transcription dynamics (pause-free velocity, pause density, pause duration) in the first nucleosomal region or the single nucleosome region. All polymerases that did not transcribe through the nucleosome in this time window were considered to be 'arrested'.

It is important to mention that our results are not sensitive to the precise value of the cutoff chosen to define passage probabilities (Fig. S4*A*). Also, qualitatively similar results are obtained without any type of selection, where, however, less of an impact of the second nucleosome onto the passage through the first one is observed, because now in some cases no nucleosomes were present (Fig. S4*B*).

Effects of the assisting force. Because in optical tweezers experiments we apply a force to the polymerase, here we explore the influence of this force on Pol II transcription dynamics in the context of a nucleosome. All transcription parameters discussed here depend to some extent on the applied force (18, 19, 21, 22). Our experiments were done in assisting force mode, where the applied force favors forward translocation of the enzyme along the DNA. In each experiment, the initial starting force was set manually to ∼12 pN with some variability around this value. When the polymerase encounters the nucleosome, the applied force is typically 9 ± 1 pN. The applied force typically decreases by ∼2 pN during nucleosomal passage. Therefore, we tested if the observed effect might be due to the effect of forces.

We therefore narrowed down the data to those trajectories that produce an average nucleosome entry force of 9 pN for each nucleosomal arrangement by discarding the extreme force values. The force range within each condition, as well as between different conditions, was therefore narrowed. Note that, as a consequence of this force threshold implementation the statistics was reduced (Fig. S5). Within the adjusted force range, possible dependencies between average transcription parameters and the average applied force were eliminated (Fig. S5 *A* and *B*). Furthermore, trends in passage probabilities for different nucleosomal templates are comparable to the trends observed for the full force range (Fig. 4*A* and Fig. S5*C*). When setting the force to 9 pN in our stochastic model, passage probabilities were still comparable to the experimental data. Therefore, we conclude that the observed differences between different nucleosomal templates predominantly arise from differences in the nucleosomal geometry rather than from the applied force.

Simulation of transcription through nucleosomes. To simulate Pol II transcription through a nucleosome we used the kinetic Monte Carlo method (23) on a 2D lattice (Fig. 2*A*). For convenience, we normalized the hopping rates (k_e, k_f, and k_b) and the cleavage rate k_{cl} by setting the largest one, which in our case is k_e, to be 1/2. At each discrete time step dt (for now $dt = 1$), we chose the direction of the next move with equal probability: if Pol II is in the active elongation mode, it can elongate 1 bp (step) further or enter a backtrack; in the backtracked state, Pol II can move forward or backward and transit to the elongation mode by the cleavage activity. Hence, the probability is one third for each direction. Next, we generated a random number r from a uniform distribution in the range $r \in [0,1)$. If the random number is smaller than the normalized rate multiplied by the number of directions, Pol II makes a step in the chosen direction; otherwise, it remains in its current position. In our Monte Carlo simulations the probability of an actual move was largest for the elongation mode and was equal to 1/2. In physical units it corresponds to k_e. Therefore, in our Monte Carlo simulations, we assigned a physical time of $(1/2k_e)$ (measured in seconds) to one time step.

In the nucleosomal region, the elongation rate (k_e) and forward hopping rate (k_f) in the backtracked state are decreased by the factor γ. In our experiments, the assisting force acting on the polymerase is typically $F_{entry} = 9 \pm 1$ pN at the entry region of the nucleosome, and it decreases by about $dF \sim 2$ pN as Pol II transcribes through the nucleosomal region (200 bp). We considered the force F to decrease linearly from the entry force. Therefore, the force F at position n bp within the nucleosome is given by $F(n) = F_{entry} - (n/200) \times dF$. For F_{entry}, we used the mean entry force of the experimental data (entry force; Table S2). Accordingly, the hopping rates k_f and k_b are changing as Pol II progresses through the nucleosomal region as $k_f(n) = k_0 \exp[+F(n)a/(k_B T)]$ and $k_b(n) = k_0 \exp[-F(n)a/(k_B T)]$. Here k_0 is the intrinsic hopping rate in the absence of force and $a = 0.17$ nm. The force can also affect the elongation rate k_e as shown in refs. 18 and 19. We estimated the variation of the k_e with F by linearly fitting the force vs. elongation rate data of previous experiments (18, 19) and found that k_e changes only by about 0.3 bp/s as the force changes by 1 pN. In our experiments, because of the narrow range of the entry force and small decrease of the force in the nucleosomal region, the change of k_e is estimated to be less than 5%. For this reason, we assume the elongation rate to be constant in our model. To simulate trajectories, we placed Pol II at the nucleosomal entry point in the elongation mode and allow it to move following the hopping rules until the time reached 145 s. We generated $\sim 10^5$ stochastic trajectories using the model parameters extracted from our experiments (Table S2). From the obtained trajectories, we then calculated passage probabilities and residence times.

The combined effect of the force and the nucleosomal barrier is reflected in the drift coefficient, $\chi = \gamma \exp[2Fa/(k_B T)]$, which is critical for the backtracking dynamics and therefore for the transcription efficiency through the nucleosomal region. Because mean entry forces vary for different DNA templates (Table S2), it is important to determine their effect on the passage probability. To address this question, in the experimental data, we choose the trajectories within a narrow range of the entry force 9.0 ± 0.8 pN for all different conditions. From these, we then determine γ (and χ). We use these parameters to simulate Pol II trajectories and calculate the passage probabilities (shown in Fig. S5*C*). The results obtained from these simulations using the narrow force range are again in agreement within errors with the experimental results for the same force range. Moreover, the trend remains the same as before when using the parameters from the full force range. We conclude, therefore, that differences in entry force between the different nucleosomal conditions are not the main factor that determines the differences in passage probabilities of different dinucleosomal configurations.

Nucleosomal Stabilities Are Comparable for the Different Dinucleosomal Templates. Because Pol II transcription dynamics were different for the different dinucleosomal templates, we wondered whether these changes can be directly attributed to differences in nucleosomal stability. To investigate the stabilities of the two neighboring nucleosomes, we performed force extension measurements for all nucleosomal templates. Experiments were done at a slow loading rate to assure that the unwrapping process occurs at equilibrium. The single nucleosome (inner wrap) unwrapped at an average force of 9.45 ± 0.45 pN (mean ± SD) at a loading rate of ∼0.5 pN/s (Fig. S7 and Table S3). This value is in good agreement with previously published data collected under similar experimental conditions (5, 30, 31). In general, we observed that unwrapping forces for the first unwrapping event were substantially lower than unwrapping forces for both the single nucleosome, as well as the second nucleosome. All dinucleosomal templates showed the same unwrapping pattern at comparable forces. Hence, stabilities of different dinucleosomal templates are comparable. We conclude, therefore, that changes in

transcription dynamics observed on different nucleosomal templates cannot be attributed to differences in nucleosomal stabilities between the different templates.

Molecular Modeling. Models were generated using Coot, make-na, and Pymol (36–38). The model is based on the following two structures: Protein Data Bank ID code 1AOI and 5C4X (2, 39).

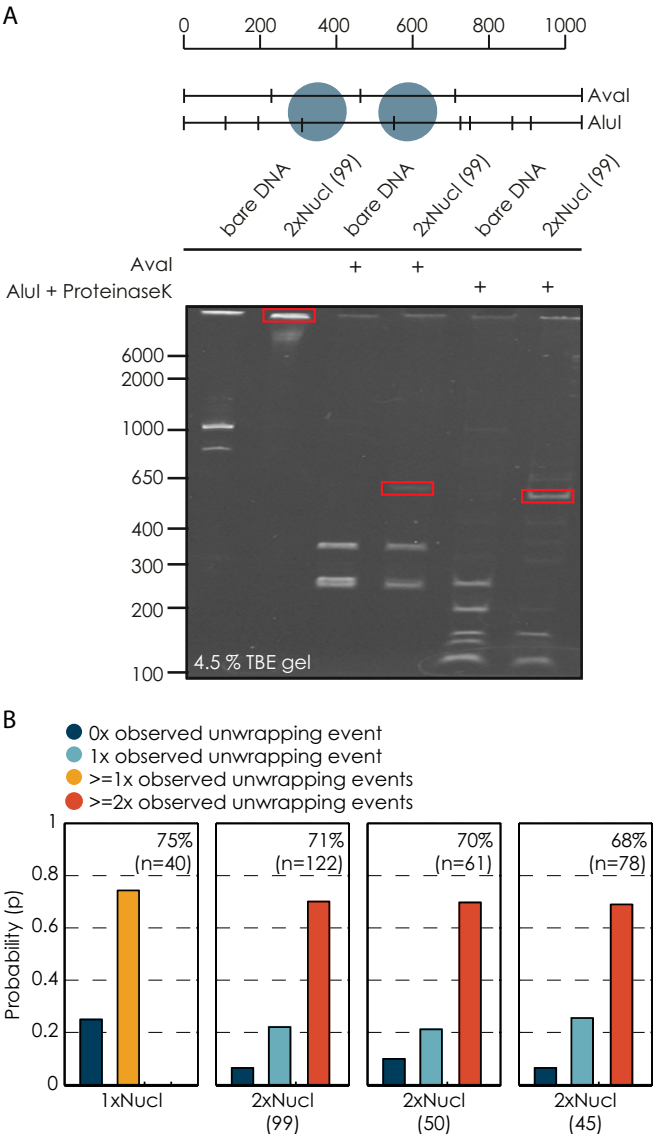

Fig. S1. Reconstitution efficiency of nucleosomal templates. (*A*) Analytical restriction digests with AvaI and AluI of the 99-bp linker DNA template. The drawing on top illustrates the cutting patterns for the 99-bp linker template for the respective enzymes. Changes in band pattern resulting from the presence of a nucleosome are highlighted in red. (*B*) Reconstitution efficiencies determined from force-extension measurements, the percentage of the number of nucleosomes found on each template. Note that in this representation one + more nucleosomal unwrapping events are binned together for the single nucleosomal condition and two + more nucleosomal unwrapping events are binned together for all dinucleosomal conditions.

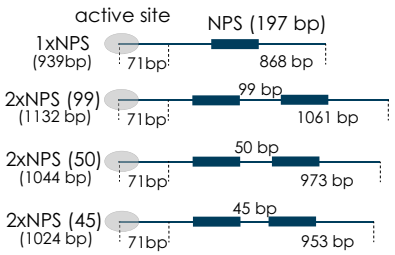

Fig. S2. Different downstream DNA templates used in this study. Illustration of different downstream templates (DNA to transcribe by Pol II in bp). The different nucleosomal templates differ in the distances between the two nucleosomes (also see *SI Text*).

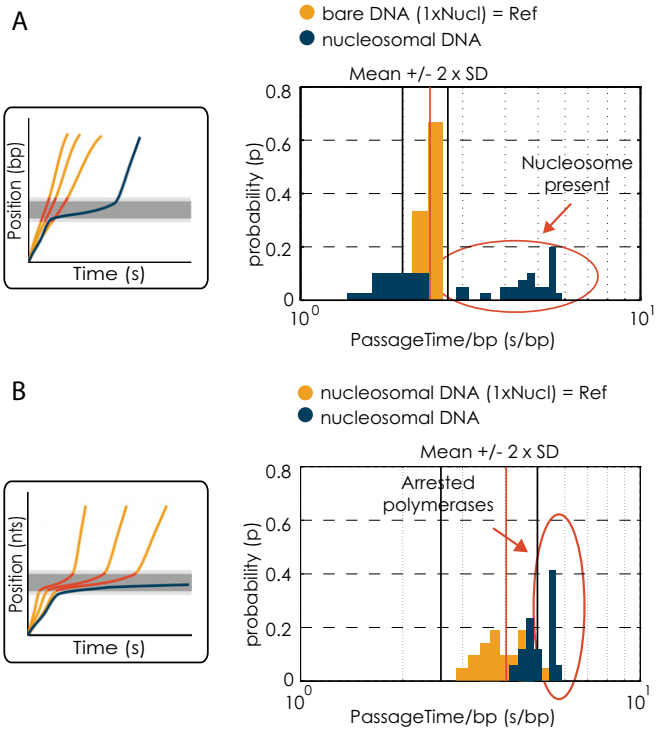

Fig. S3. Data quality check for the presence of a nucleosome and sufficient nucleosomal residence time. (*A*) Quality check for presence of a nucleosome. (*Left*) Schematic of the data quality check method. The gray bar indicates the position of the nucleosome. The cutoff for determining the presence of a nucleosome was derived from transcription trajectories on bare DNA within the nucleosomal region (red). The blue line corresponds to a trajectory on a single nucleosomal template. (*Right*) The passage time distribution for the first nucleosome of the dinucleosomal template (50-bp linker) (blue). The yellow bars show the reference distribution of the bare DNA. All passage times longer than the cutoff (mean + 2 × SD = 11.2 + 2 × 1.9 s) are considered to result from the presence of a nucleosome. The *x* axis is in logarithmic scale. (*B*) Quality check for long enough residence times within the first nucleosomal region. (*Left*) Schematic of the data quality check method. The gray bar indicates the position of the nucleosome. The cutoff for selecting for sufficient nucleosomal residence time for all polymerases that did not make it through the nucleosomal region was derived from residence times of transcription trajectories on single nucleosomal templates within the nucleosomal region (red). The blue line represents a trajectory of a polymerase ending within the nucleosomal region. (*Right*) The passage time distribution for the first nucleosome of the dinucleosomal template (50-bp linker) for all runs that ended in the respective region (blue). The yellow bars show the reference distribution of the single nucleosomal template. All passage times longer than the cutoff (mean + 2 × SD = 66.04 + 2 × 39.68 s) are considered for further analysis. The *x* axis is in logarithmic scale.

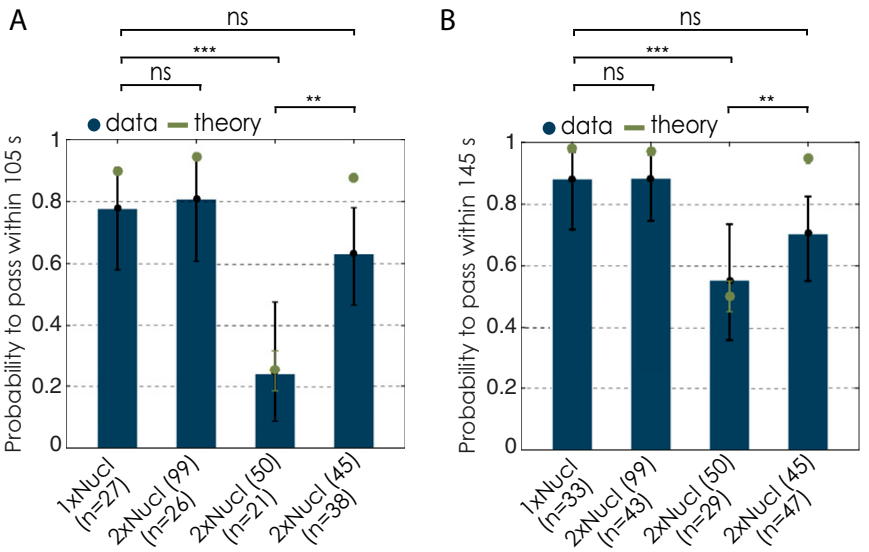

Fig. S4. Changes in passage probabilities with different evaluation criteria. (*A*) Passage probabilities within 105 s (mean + 1 SD of the nucleosomal residence time). The error bars represent 95% CI. Experimental data are shown in blue; theory is shown in green. (*B*) Passage probabilities for all data before selecting for the presence of the first nucleosome. Note that for polymerases arrested within the first nucleosomal region, only transcription trajectories with an arrest length above 145 s were considered. Furthermore, for the analysis of Pol II transcription dynamics of all data, we also considered only 145 s after encountering the nucleosome. We used the Barnard's exact test to calculate the *P* values for binary data sets. Two datasets are considered significantly different if the *P* value is below or equal to 0.05. Different *P* values are indicated as follows: ns, $P > 0.05$; $^{**}P \leq 0.01$; and $^{***}P \leq 0.001$.

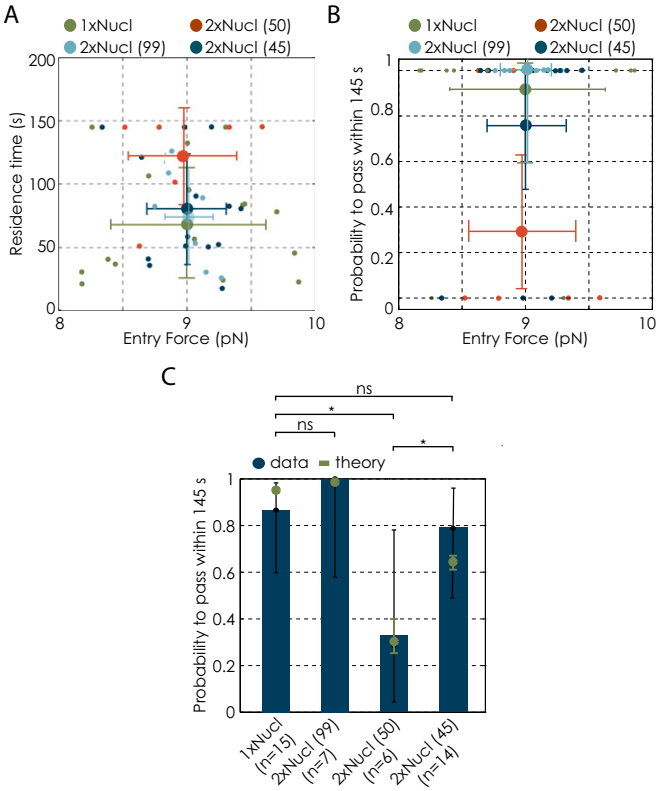

Fig. S5. Influence of applied force on Pol II transcription behavior. (*A*) Relationship between residence times and the applied force for all conditions for the defined average entry force of 9.0 pN. Data are shown as mean ± SD. (*B*) Relationship between passage probabilities and the applied force for all conditions for the defined average entry force of 9.0 pN. Force data are shown as mean ± SD. Error bars for passage probabilities represent 95% CI. Small dots represent single experiments (*A* and *B*). (*C*) Changes in passage probabilities between different conditions for the defined average entry force of 9.0 pN. Theory (green) was done for an entry force of 9.0 pN. Error bars represent 95% CI. We used the Barnard's exact test to calculate the *P* values for binary datasets. Two datasets are considered significantly different if the *P* value is below or equal to 0.05. Different *P* values are indicated as follows: ns, $P > 0.05$; $^{*}P \leq 0.05$;

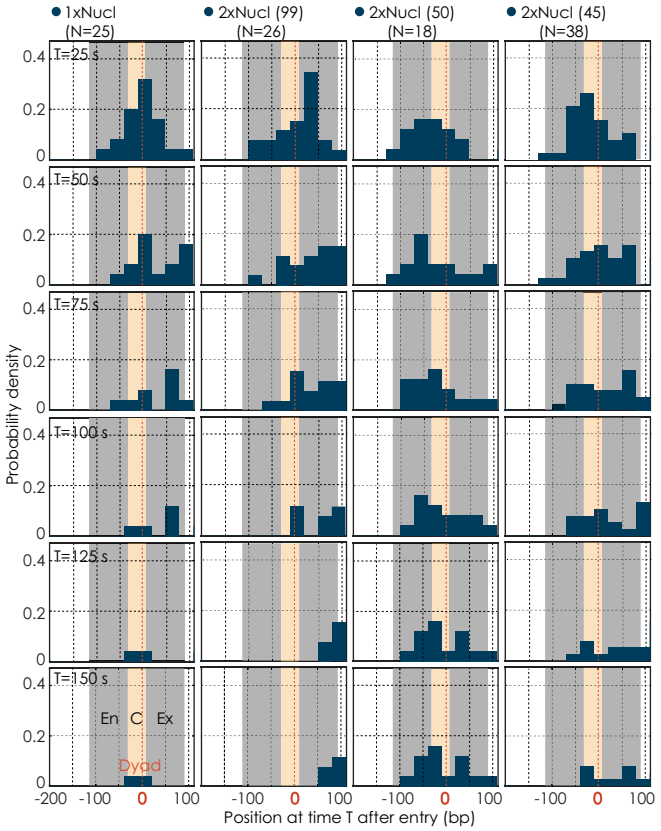

Fig. S6. Time evolution of nucleosomal transcription along different nucleosomal templates. Probability densities of polymerases within the first nucleosomal region at different time points (T) during nucleosome transcription. The time points are taken 25 s apart from each other. The gray bar illustrates the position of the first nucleosome (En, entry; Ex, exit); the yellow area marks the central region (C, central). *N* indicates the number of Pol II transcription trajectories on each template.

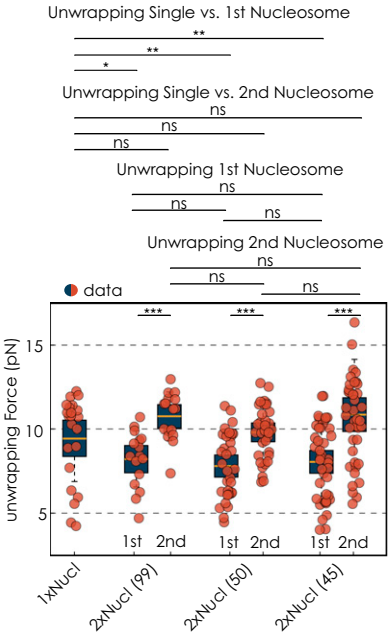

Fig. S7. Nucleosomal stabilities for different nucleosomal templates. Distributions of unwrapping forces are splitted into the first and the second nucleosomal unwrapping event. Unwrapping forces are in general higher for the second unwrapping event. Quantifications for the unwrapping forces for the different conditions are shown as box plots, where the central mark is the median, the edges of the box are the 25th and 75th percentiles, and the whiskers extend to the most extreme data points not considered outliers. The red dots represent values for single experiments. We used the Wilcoxon rank sum test to compare two sets of data. Two datasets are considered significantly different if the *P* value is below or equal to 0.05. Different *P* values are indicated as follows: ns, $P > 0.05$; *$P \leq 0.05$; **$P \leq 0.01$; and ***$P \leq 0.001$.

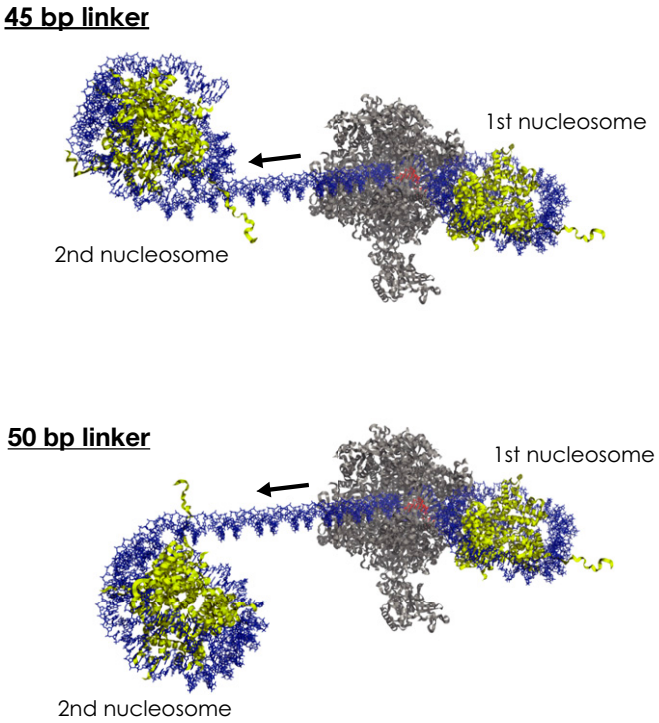

Fig. S8. Molecular models for the different nucleosomal geometries: Two models with a 45- or 50-bp linker illustrate the angular distribution of two neighboring nucleosomes in the presence of an elongating RNA polymerase II complex. Pol II is situated in the exit side (past the dyad) of the first nucleosome. The black arrow indicates the direction of transcription. RNA polymerase II is rendered in gray, histone octamer in yellow, DNA in blue, and RNA in red. Models were generated using Coot and Pymol.

Table S1. Transcription parameters for all conditions

Template	Residence times (s)	Pause-free velocity (bp/s)	Pause density (pauses/kbp)	Pause duration (s)	Passage probability (%)
Bare DNA	10.3 ± 1.4 (10.2)	24.7 ± 4.1 (23.3)	4.6 ± 2.8 (5.0)	2.0 ± 0.7 (1.8)	100.0
1×Nucl	63.5 ± 15.5 (48.0)	16.5 ± 2.5 (15.6)	24.6 ± 5.8 (20.0)	12.0 ± 3.2 (9.1)	92.0
2×Nucl (99)	69.8 ± 16.5 (64.2)	16.3 ± 1.9 (15.6)	23.4 ± 5.1 (20.0)	12.0 ± 3.7 (10.9)	92.3
2×Nucl (50)	118.9 ± 23.0 (145.0)	12.3 ± 1.8 (11.2)	38.6 ± 8.3 (41.3)	37.9 ± 19.2 (23.0)	27.8
2×Nucl (45)	83.3 ± 15.1 (83.9)	15.6 ± 1.8 (14.6)	28.4 ± 5.2 (25.0)	15.9 ± 4.0 (13.9)	78.9

*All quantities are reported as mean ± SEM The median is given in parentheses.

Table S2. Parameters used in the model

Template	γ	Entry force (pN)	χ*	k_0 (1/s)*
1×Nucl	0.67 ± 0.11	9.5 ± 1.0	1.35 ± 0.25	0.56 ± 0.14
2×Nucl (99)	0.67 ± 0.12	10.4 ± 1.2	1.46 ± 0.30	0.55 ± 0.12
2×Nucl (50)	0.48 ± 0.12	8.2 ± 0.8	0.87 ± 0.22	0.61 ± 0.13
2×Nucl (45)	0.63 ± 0.14	9.7 ± 0.7	1.29 ± 0.30	0.61 ± 0.11

*Values are obtained by using the force in the middle of the nucleosome, i.e., entry force − 1 pN.

Table S3. Average unwrapping forces for the inner wrap of all nucleosomal conditions

Template	UW force first Nucl*	UW force second Nucl
1×Nucl	9.5 ± 2.6 (10.7)	
2×Nucl (99)	8.2 ± 1.7 (8.4)	10.8 ± 1.4 (11.2)
2×Nucl (50)	7.8 ± 1.9 (7.6)	9.8 ± 1.6 (9.9)
2×Nucl (45)	8.1 ± 2.2 (8.2)	10.8 ± 3.3 (10.8)

*Quantity reported as mean ± SD. The median is given in parentheses.